Precision Measurements in Helium at 58 nm: Ground State Lamb Shift and the 1^1S-2^1P Transition Isotope Shift

K. S. E. Eikema, W. Ubachs, W. Vassen, and W. Hogervorst

Laser Centre Vrije Universiteit, Department of Physics and Astronomy, De Boelelaan 1081, 1081 HV Amsterdam, The Netherlands

(Received 1 May 1995; revised manuscript received 18 September 1995)

A source of narrow bandwidth (<800 MHz) tunable laser radiation at 58.4 nm has been developed and is applied to record the 1^1S-2^1P transition in ^{3}He and ^{4}He. From the ^{4}He transition frequency of 171 134.8936(58) cm^{-1} a fivefold improved ground state Lamb shift of 1.3763(58) cm^{-1} is deduced, in good agreement with the theoretical value of 1.3755(10) cm^{-1}. The measured 1^1S-2^1P transition isotope shift of 263 410(7) MHz presents a more than 2 order of magnitude improvement over a previous value and agrees with a theoretical value of 263 411.26(11) MHz.

PACS numbers: 32.30.Jc, 12.20.Fv, 42.65.Ky

Until recently high resolution spectroscopy in the extreme ultraviolet (XUV), in particular, at wavelengths below 90 nm, has been hampered by lack of light sources with sufficiently narrow bandwidth. Although synchrotron sources do generate XUV radiation, their large bandwidth prevents measurements at the required accuracy level even in combination with sophisticated monochromators [1]. An important application of a narrow-band XUV source is the study of the ground state transition 1^1S-2^1P at 58 nm in the helium atom, where recent theoretical calculations of level energies [2] have stimulated new experimental investigations. Lamb shift measurements in helium provide a stringent test of quantum electrodynamics (QED) including two-electron effects, whereas isotope shift measurements may yield values for the difference in nuclear charge radius of ^{3}He and ^{4}He. The inaccessibility of the 58 nm wavelength range has hitherto prevented a study of Lamb shift and isotope effects in the ground state transition, although they are an order of magnitude larger than in any other transition. For this reason several groups studied transitions from the 2^1S_0 and 2^3S_1 metastable states to 3^1P, 2^3P, and 3^3P states [3–6].

Recently, we succeeded in the generation of tunable radiation at wavelengths as short as 58 nm by fifth-harmonic conversion of the output of a frequency-doubled pulsed dye laser [7]. In this feasibility experiment we demonstrated that ^{4}He can be excited with narrow-band coherent XUV radiation at 58.4 nm. It resulted in a fivefold improved value of the 1^1S Lamb shift (1.38 ± 0.03 cm^{-1}). This result encouraged us to design and build a much improved experimental setup for precision spectroscopy at the MHz level in the XUV. Again it is applied to study the 1^1S-2^1P transition in He and, in particular, to measure the ground state Lamb shift as well as the isotope shift. The Lamb shift of the ground state is deduced from the measured absolute transition frequency using the accurately known energy of 2^1P and the non-QED energy of the ground state (see [7] and [8]). The best value for the 1^1S-2^1P isotope shift thus far was obtained in a classical emission experiment by Herzberg in 1958 with an accuracy of 1.8 GHz [9].

In Fig. 1 a schematic of the new experimental setup is given. The fundamental frequencies in the experiment are produced with a continuous wave (CW) ring laser operating at 584 nm on the dye Rhodamine 6G. Accurate frequency markers are obtained with an etalon, which is sealed, temperature stabilized, and locked to a 632.8 nm HeNe laser, which itself is locked to a hyperfine component of I_2. This ensures a reproducible free spectral range (FSR) of 148.9567(4) MHz, and negligible drift during frequency scans of the laser. Calibration of the etalon is based on frequency standards [10,11] measured with saturation spectroscopy in I_2. Absolute calibration of the ^{4}He transition is based on the I_2 line at 513 049 427(3) MHz indicated in Fig. 2 with an asterisk. This I_2 hyperfine component was calibrated in our laboratory using the i component of R(99)15-1 from [11]. The CW laser output is coupled into a single mode fiber to transport the laser light to a home-built high power pulse-dye amplifier (PDA) containing Rhodamine B. The amplifier, pumped by 650 mJ at 532 nm from an injection-seeded Nd:YAG laser with a repetition rate of 10 Hz, generates 200 mJ of light at 584 nm in a 5.5 ns pulse with a bandwidth of 95 MHz. Frequency doubling of this output in a KD*P crystal produces on average 90 mJ/pulse at 292 nm (~5 ns). The UV is separated from the visible light and focused with a 29 cm lens in an expanding, pulse gas jet of C_2H_2 for nonlinear up-conversion. At least 10^5 photons per laser shot around 58 nm are produced at the fifth harmonic.

To reduce Doppler effects this experiment is performed in a crossed atomic-beam-laser setup (see Fig. 1). In an interaction chamber the diverging UV and XUV beams perpendicularly intersect a skimmed and pulsed beam of helium seeded in krypton (5% ^{3}He, 5% ^{4}He, and 90% Kr). This seeding in krypton conveniently reduces the velocity of both helium isotopes to the same value. Once excited from the ground state to the 2^1P state by an XUV photon (absorption less than a few percent), the

 0031-9007/96/76(8)/1216(4)$06.00

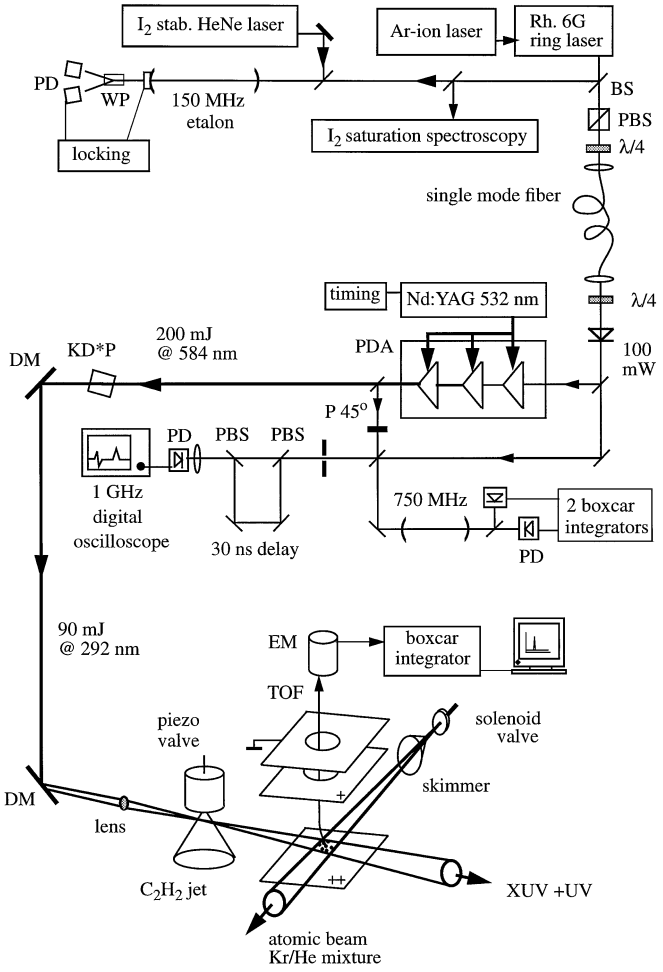

FIG. 1. Schematic of the experimental setup (UV is ultraviolet, XUV is extreme ultraviolet, PD is photodiode, PDA is pulse dye amplifier, EM is electron multiplier, TOF is time-of-flight tube, VIS is visible light, DM is dichroic mirror, PBS is polarizing beam splitter, and P is polarizer).

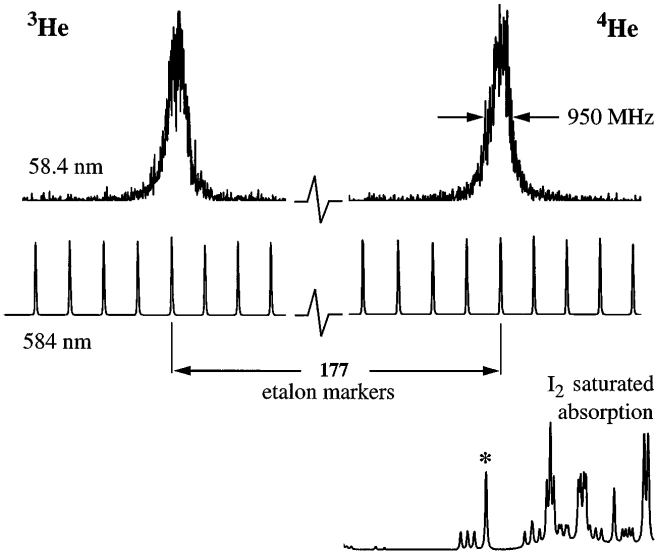

FIG. 2. Typical isotope shift measurement in the 1^1S-2^1P transition at 58.4 nm (upper part). Each data point is an average over four laser shots at fixed frequency. The full width at half maximum of the resonance lines consists of ~60 data points. The middle and lower parts show, respectively, the fringes of the 150 MHz calibration etalon and a saturated absorption spectrum of I_2. The peak indicated with an asterisk is used for absolute frequency calibration (see text).

powerful UV ionizes approximately 10% of the excited atoms. A delayed and pulsed electric field is then used to extract these ions from the interaction zone to an electron multiplier for detection. Figure 2 shows a typical example of such a measurement with etalon frequency markers and an I_2 saturation spectrum.

Measurements have been performed with a 2 mm diameter circular skimmer as well as with a 5×1 mm slit skimmer, 10 cm from the nozzle orifice. The calibration was interpolated with a cubic spline between the etalon frequency markers. The intensity and position of the helium resonances were fitted with skewed Voigt profiles, and no significant differences in peak shapes were found for ^{3}He and ^{4}He resonances or for the measurements with both skimmers. A weighted average over 17 measurements results in a 1^1S-2^1P transition frequency for ^{4}He of 171 134.8946 cm^{-1} (5 130 495 070 MHz) and a ^{4}He-^{3}He isotope shift of 263 416 MHz (see Table I). The statistical error in the absolute calibration is 7 MHz. A careful analysis of the statistical error in the weighted average of the isotope shift measurements gives a value of 3.2 MHz. We increase it to 5 MHz to account for possible uncertainties in error distribution and shape parameter differences between ^{3}He and ^{4}He.

The three main sources of systematic error are Doppler shifts, time dependent laser frequency (chirp) due to the pulse dye amplification process, and the subsequent nonlinear up-conversion, and dynamic (or ac) Stark shift due to the high UV power in the interaction volume. Also the unresolved hyperfine structure of ^{3}He (nuclear spin $I = \frac{1}{2}$) has to be considered. Pressure effects are excluded because excitation occurs in an atomic beam.

To assess the Doppler error, the velocity difference between beams of pure ^{4}He and ^{4}He seeded in krypton [1200(300) vs 480(100)m/s] has been used to determine the angle between the atomic beam and XUV beam. Minimization of the measured Doppler shift difference between both situations relative to the I_2 hyperfine components shown in Fig. 2 allows the beams to be perpendicularly aligned within 0.2 deg. This results in a 30 MHz Doppler error for the absolute calibration. From a calculated maximum Doppler width of ~300 MHz (based on skimmer-nozzle geometry), a natural linewidth of 300 MHz, and an estimated XUV radiation bandwidth ~300 MHz (based on the bandwidth of the PDA system in the visible as well as on chirp)

TABLE I: Experimental and theoretical values for the 1^1S-2^1P transition frequency and ^{4}He-^{3}He isotope shift, with their 1σ errors. All numbers in MHz.

	Isotope shift	1^1S-2^1P of ^{4}He
Uncorrected value	263 416	5 130 495 070
Corrections:		
ac Stark shift	−6	−80
Chirp	—	+50
Corrected values	263 410(7)	5 130 495 040(175)
Theory	263 411.26(11)	5 130 495 064(30)
Error budget (1σ)*:*		
Statistical	5	7
ac Stark shift	3	40
Doppler shift	2	30
Chirp	—	150
Asymmetry	3	70
Calibration	1	30
rms error	7	175

we expected an experimental linewidth of ~500 MHz. However, we observed a linewidth of 950 MHz. Probably due to collisions with atoms, backscattered from the skimmer, the divergence of the atomic beam is larger than estimated; this might be responsible for the slightly asymmetric line profile as well. The asymmetry, which cannot be explained by chirp effects (see below), causes an additional uncertainty of 70 MHz in the absolute calibration. From the measured linewidth an XUV radiation bandwidth smaller than 800 MHz is deduced. For the isotope shift any residual velocity difference between ^{3}He and ^{4}He (seeded in krypton) combined with the 0.2 deg uncertainty in the angle between the XUV and helium beam may also result in a Doppler error. The magnitude of this effect is estimated by comparing measurements of the isotope shift at an angle of 87.2(2)° [263 402(15) MHz] with the measurements at 90° alignment. In this way a Doppler shift uncertainty of 2 MHz in the isotope shift is deduced. Other Doppler related error sources for the isotope shift may be due to differences for ^{3}He and ^{4}He in the XUV or UV intensity profile, atomic density, and angular density distribution. Those effects have been estimated and listed in Table I under "asymmetry."

The second source of error, frequency chirp, is a result of phase modulation caused by time dependent refractive indices in each stage of the conversion process from CW light to XUV. Contributions to chirp may arise from time dependent gain (in the PDA [12]), nonlinear refractive index and phase mismatch (in the frequency doubling [13]), and time dependent refractive index due to excitation or ionization (in the fifth-harmonic generation). Although chirp generally depends on wavelength [12], it is equal for ^{3}He and ^{4}He as only a small (<1 cm^{-1}) wavelength excursion in the visible is involved and can therefore be ignored for the isotope shift. In order to reduce systematic errors in the isotope shift induced by slow time dependent changes (changes in chirp due to dye degradation, but also, e.g., beam disalignment), we performed measurements in alternating pairs of ^{3}He and ^{4}He. These effects, if present, will then be averaged out to first order in the isotope shift and only contribute to the statistical error. Absolute calibration, however, is most susceptible to chirp effects from the pulse dye amplification. We measured this effect with a method similar to the one used in Ref. [13], by recording the time dependent interference between the CW and PDA output beams on a 1 mm diaphragm with a fast photodiode (see Fig. 1). Opposite polarizations are used to record both the interference term and the intensity of the pulsed beam. Taking into account the contrast of the interference signal the phase of the PDA output and therefore the instantaneous frequency difference with the CW seed beam can be reconstructed. In combination with an etalon measurement of the average frequency difference between pulsed and CW beams the sign of the chirp is deduced. The XUV production process selects the high intensity central part of the pulse, where the frequency excursion on average ranges from +15(3) in the first half to −25(5) MHz at the second half of the pulse (with a zero crossing 1 ns after the intensity maximum). The effect of this chirp in the XUV transition has been calculated using the optical Bloch equations. For this purpose we measured the UV intensity on PDA output dependence (power 1.15) and the XUV intensity dependence on UV (fourth power). On average a shift of −50(150) MHz in the XUV resonance frequency with respect to 10 times the CW laser frequency is calculated. The large error in this shift is due to the uncertainty in the actual chirp and beam characteristics during the XUV measurements. Chirp effects in the frequency doubling process are estimated to be negligible under our experimental conditions [13]. By changing the C_2H_2 density over a considerable XUV signal range no indication of chirp or linewidth broadening in the fifth-harmonic conversion process was found. Similar test measurements with Xe as the fifth-harmonic conversion medium showed strong broadening (up to 2.5 GHz) and severe shifts (up to 400 MHz) starting immediately after the first visible signs of breakdown. More details of the chirp measurements and calculations will be given in a future publication.

The third error source is a dynamic Stark shift. It has been evaluated for a central peak UV intensity of 25 MW/cm^2, based on the assumption that the XUV beam is well confined within the spatial and temporal dimensions of the fundamental UV radiation. The XUV intensity of a

few mW/cm^2 is negligible in this respect. For ^{4}He a total shift of 80(40) MHz is calculated, which has to be subtracted from the measured transition frequency. Because of the hyperfine structure in ^{3}He, the dynamic Stark shift is slightly smaller for ^{3}He compared to ^{4}He. Only the polarizability of the 2^1P state is isotope dependent and has to be considered for the isotope shift. The calculated absolute Stark shift of ~75 MHz for the 2^1P level is comparable to the hyperfine splitting of 41.7 MHz between the $F = \frac{1}{2}$ and $F = \frac{3}{2}$ components. Therefore the combined effect must be calculated by diagonalizing the Stark, fine, and hyperfine interactions together in the $1s2p$ configuration in a $|LSJIFM_F\rangle$ basis. The transition frequency of ^{4}He can be calculated directly from the dynamic scalar and tensor polarizabilities; for ^{3}He, however, the center of gravity has to be calculated for the unresolved and therefore coherently excited 2^1P $F = \frac{1}{2}$ and $F = \frac{3}{2}$ states. Details of this calculation will be published elsewhere. The combined effect of hyperfine structure and dynamic Stark shift is a 6(3) MHz reduction of the measured isotope shift.

Incorporating all corrections we obtain an absolute transition frequency for ^{4}He of 171 134.8936(58) cm^{-1} and an isotope shift of 263 410(7) MHz. From the absolute transition frequency measurement a new value of 1.3763(58) cm^{-1} for the ground state Lamb shift of ^{4}He is deduced. This value is a fivefold improvement over our previous result [7], and is in good agreement with the theoretical value of 1.3755(10) cm^{-1} [2,8]. The 0.001 cm^{-1} error in the theoretical value is due to several, not yet calculated, QED contributions of $O(\alpha^4)$ or higher. The isotope measurement presents a more than 2 order of magnitude improvement over the value of 264.6(1.8) GHz obtained by Herzberg [9]. Theoretically an isotope shift of 263 411.26(11) MHz is deduced from the most recent variational calculations including QED corrections [2,14] and the latest values for the nuclear charge radii of ^{3}He and ^{4}He [6]. Our experimental value is in excellent agreement with the thus calculated isotope shift.

Our experiments in the extreme ultraviolet range of the spectrum demonstrate that precision spectroscopy near 58 nm is possible now with an unprecedented accuracy. An absolute frequency accuracy of 3 parts in 10^8 in the XUV has been achieved. A measurement of the ground state Lamb shift with an accuracy approaching the accuracy of the theoretical calculations (30 MHz) seems feasible, although frequency chirp effects provide a serious challenge. Work to assess and reduce the importance of frequency chirp effects in our XUV source is in progress.

We gratefully acknowledge financial support of the Foundation for Fundamental Research on Matter (FOM), which is part of the Netherlands Organization for the Advancement of Research (NWO).

[1] K. Ito, T. Namioka, Y. Morioka, T. Sasaki, H. Noda, K. Goto, T. Katayama, and M. Koike, Appl. Opt. **6**, 837 (1986).
[2] W. F. Drake, *Long-Range Casimir Forces: Theory and Recent Experiments on Atomic Systems*, edited by F. S. Levin and D. A. Micha (Plenum Press, New York, 1993).
[3] W. Lichten, D. Shiner, and Zhi-Xiang Zhou, Phys. Rev. A **43**, R1663 (1991).
[4] D. Shiner, R. Dixson, and P. Zhao, Phys. Rev. Lett. **72**, 1802 (1994).
[5] F. Marin, F. Minardi, F. S. Pavone, M. Inguscio, and G. W. F. Drake, Z. Phys. D **32**, 285 (1995). Table 4 contains a misprint: C_0 for the $^1P_1$ should read −4285.829 MHz [G. W. F. Drake (private communication)].
[6] D. Shiner, R. Dixson, and V. Vedantham, Phys. Rev. Lett. **74**, 3553 (1995).
[7] K. S. E. Eikema, W. Ubachs, W. Vassen, and W. Hogervorst, Phys. Rev. Lett. **71**, 1690 (1993).
[8] G. W. F. Drake, I. B. Khriplovich, A. I. Milstein, and A. S. Yelkhovsky, Phys. Rev. A **48**, R15 (1993).
[9] G. Herzberg, Proc. R. Soc. London A **248**, 309 (1958).
[10] L. Hlousek and W. M. Fairbank Jr., Opt. Lett. **8**, 322 (1983).
[11] R. Grieser, G. Bönsch, S. Dickopf, G. Huber, R. Klein, P. Merz, A. Nicolaus, and H. Schnatz, Z. Phys. A **348**, 147 (1994).
[12] N. Melikechi, S. Gangopadhyay, and E. E. Eyler, J. Opt. Soc. Am. B **11**, 2402 (1994).
[13] S. Gangopadhyay, N. Melikechi, and E. E. Eyler, J. Opt. Soc. Am. B **11**, 231 (1994).
[14] G. W. F. Drake (private communication).